Article

Effective Modulation of DNA Duplex Stability by Reversible Transition Metal Complex Formation in the Minor Groove

Marcin Kalek, Andreas S. Madsen, and Jesper Wengel

J. Am. Chem. Soc., **2007**, 129 (30), 9392-9400• DOI: 10.1021/ja071076z • Publication Date (Web): 07 July 2007

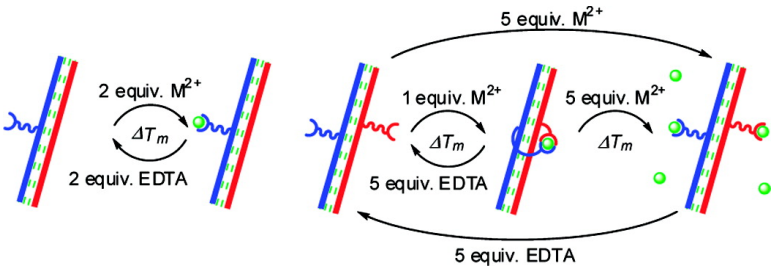

More About This Article

Additional resources and features associated with this article are available within the HTML version:

- Supporting Information
- Links to the 7 articles that cite this article, as of the time of this article download
- Access to high resolution figures
- Links to articles and content related to this article
- Copyright permission to reproduce figures and/or text from this article

View the Full Text HTML

J|A|C|S
ARTICLES
Published on Web 07/07/2007

Effective Modulation of DNA Duplex Stability by Reversible Transition Metal Complex Formation in the Minor Groove

Marcin Kalek,[†] Andreas S. Madsen, and Jesper Wengel*

Contribution from the Nucleic Acid Center,[‡] Department of Physics and Chemistry, University of Southern Denmark, DK-5230 Odense M, Denmark

Received February 14, 2007; E-mail: jwe@ifk.sdu.dk

Abstract: Herein we describe the reversible changing of DNA duplex thermal stability by exploiting transition metal complexation phenomena. A terpyridine ligand was conjugated to the N2′-atoms of 2′-amino-2′-deoxyuridine and its locked counterpart 2′-amino-LNA, and these metal-complexing monomers were incorporated into oligodeoxyribonucleotides. Upon addition of varying amounts of transition metal ions, the thermal stability of DNA duplexes containing these terpyridine-functionalized units in different constitutions was affected to different degrees (ΔT_m values = −15.5 to +49.0 °C, relative to the unmodified duplex). The most pronounced effects were observed when two complexing monomers were positioned in opposite strands. Addition of 1 equiv of Ni^{2+} to such a system induced extraordinary duplex stabilization. Molecular modeling studies suggest, as an explanation for this phenomenon, formation of nickel-mediated interstrand linkages in the minor groove. Addition of an excess of metal ions resulted in largely decreased T_m values. Alternating addition of metal ions and EDTA demonstrated reversibility of metal ion-induced changes in hybridization strength, proving that the described approach provides an efficient method for duplex stability modulation.

Introduction

DNA, with its ability to form well-defined, three-dimensional structures, is considered to be a suitable material for construction of self-assembling, nanoscale devices.[1−5] Due to sequence-specific duplex formation, according to the Watson−Crick base-pairing rules, it is possible to create almost any desired supramolecular motif.[6] However, once such a system has been assembled, it cannot, in the majority of cases, be further changed. Finding methods to control DNA folding in effective and reversible ways is a challenging task, but, successfully accomplished, it would open completely new possibilities in nanotechnology. There have been only a few attempts to address this issue. These include application of aptamers, which selectively "remove" given DNA strands from the system,[7] caged oligonucleotides (ONs), which become capable of duplex formation only after photoirradiation,[8] and ONs containing linkers that may be cleaved with a selective reagent.[7] In the course of our studies on modulation of the hybridization process using modified ONs, we turned our attention to conjugates of nucleic acids with metal-chelating moieties. We believe that these systems will create an orthogonal way to manipulate DNA folding and, as such, expand the potential of DNA-based nanotechnology.

The ability to form complexes of defined structure is a well-known property of transition metal ions. It has been widely exploited to construct many self-assembling nanostructures.[9] In the past decade, several groups have furthermore reported preparation of modified DNA duplexes in which the natural Watson−Crick hydrogen bonding has been replaced with metal-mediated base pairing.[10] However, locating metal ions in the core of the helix, even though it changes the duplex stability, is rather aimed at creating metal nanowires than at regulation of DNA folding.[11] The only exception to this tendency was the

[†] Current affiliation: Department of Organic Chemistry, Arrhenius Laboratory, Stockholm University, 106 91 Stockholm, Sweden.

[‡] A research center funded by the Danish National Research Foundation for studies on nucleic acid chemical biology.

(1) Simmel, F. C.; Yurke, B. *Appl. Phys. Lett.* **2002**, *80*, 883−885.
(2) Liu, D.; Shankar, B. *Angew. Chem. Int. Ed.* **2003**, *42*, 5734−5736.
(3) Gothelf, K. V.; LaBean, T. H. *Org. Biomol. Chem.* **2005**, *3*, 4023−4037.
(4) Liao, S.; Seeman, N. C. *Science* **2004**, *306*, 2072−2074.
(5) Sherman, W. B.; Seeman, N. *Nano Lett.* **2004**, *4*, 1203−1207.
(6) Feldkamp, U.; Niemeyer, C. M. *Angew. Chem. Int. Ed.* **2006**, *45*, 1856−1876.
(7) Miduturu, C. V.; Silverman, S. K. *Angew. Chem. Int. Ed.* **2006**, *45*, 1918−1921.
(8) Höbartner, C.; Silvermann, S. K. *Angew. Chem. Int. Ed.* **2005**, *44*, 7305−7309.
(9) Leininger, S.; Olenyuk, B.; Stang, P. J. *Chem. Rev.* **2000**, *100*, 853−908.
(10) (a) Meggers, E.; Holland, P.; Tolman, W. B.; Romesberg, F. E.; Schultz, P. G. *J. Am. Chem. Soc.* **2000**, *122*, 10714−10715. (b) Atwell, S.; Meggers, E.; Spaggon, G.; Schultz, P. G. *J. Am. Chem. Soc.* **2001**, *123*, 12364−12367. (c) Zimmermann, N.; Meggers, E.; Schultz, P. G. *J. Am. Chem. Soc.* **2002**, *124*, 13684−13685. (d) Zimmermann, N.; Meggers, E.; Schultz, P. G. *Bioorg. Chem.* **2004**, *32*, 13−25. (e) Zhang, L.; Meggers, E. *J. Am. Chem. Soc.* **2005**, *127*, 74−75. (f) Kentaro, T.; Tasaka, M.; Cao, H.; Shionoya, M. *Supramol. Chem.* **2002**, *14*, 255−261. (g) Tanaka, T.; Tengeiji, A.; Shionoya, M. *J. Am. Chem. Soc.* **2002**, *124*, 8802−8803. (h) Tanaka, T.; Tengeiji, A.; Kato, T.; Toyama, N.; Shiro, M.; Shionoya, M. *J. Am. Chem. Soc.* **2002**, *124*, 12494−12498. (i) Switzer, C.; Shin, D. *Chem. Commun.* **2005**, 1342−1344. (j) Switzer, C.; Shina, S.; Kim, P. H.; Heuberger, B. D. *Angew. Chem. Int. Ed.* **2005**, *44*, 1529−1532. (k) Weizman, H.; Tor, Y. *J. Am. Chem. Soc.* **2001**, *123*, 3375−3376. (l) Brotschi, C.; Leumann, C. J. *Nucleosides Nucleotides Nucleic Acids* **2003**, *22*, 1195−1197. (m) Clever, G. H.; Polborn, K.; Carell, T. *Angew. Chem. Int. Ed.* **2005**, *44*, 7204−7208. (n) Miyake, Y.; Togashi, H.; Tashiro, M.; Yamaguchi, H.; Oda, S.; Kudo, M.; Tanaka, Y.; Kondo, Y.; Sawa, R.; Fujimoto, T.; Machinami, T.; Ono, A. *J. Am. Chem. Soc.* **2006**, *128*, 2172−2173.
(11) Tanaka, K.; Tengeiji, A.; Kato, T.; Toyama, A.; Shionoya, M. *Science* **2003**, *299*, 1212−1213.

10.1021/ja071076z CCC: $37.00

preparation of a mercury(II) sensor by Ono and co-workers, who took advantage of the high stability of Hg^{2+}-mediated T−T base pairs.[12] On the other hand, a large number of nucleotide building blocks positioning metal chelators outside the DNA duplex, in either the major or the minor groove, have been synthesized.[13,14] This group of compounds was employed mainly to obtain so-called artificial ribonucleases, catalyzing sequence-specific RNA cleavage.[15,16]

Pursuing a way of changing the stability of the duplex, depending on the presence or absence of transition metal ions, we designed a system with metal chelators located outside the helix core and positioned toward the minor grove of the duplex. We believe, as far as duplex stability modulation is concerned, that conjugates of DNA containing the metal-complexing moiety outside the duplex core are advantageous over those with internally placed metal-coordinating base pairs. First, the complex should be easily accessible, so that both introduction and extraction of the metal ion will not require full denaturation of the duplex. Second, transition metal ions located in one of the grooves have the possibility to interact with the phosphate backbone, as well as with adjacent nucleobases, and may, in this way, have additional influence on the stability of the system.[17−21] Finally, by keeping the natural base pairing intact, Watson−Crick mismatch discrimination is not compromised. Recent results support the above-mentioned considerations and prove the usefulness of metal complex-based control of DNA duplex stability and folding.[14,22−24]

The proposed mechanism of metal-induced duplex stability change is illustrated in Figure 1. When the metal-coordinating moiety is incorporated into only one of the DNA strands (Figure 1, structure A), addition of metal ion and the resulting complexation (Figure 1, structure B) may change the stability of the system due to different interactions, such as the above-mentioned stabilization of the negatively charged phosphate backbone or co-complexation by the heteroatoms of the nucleobases.[17] More dramatic effects can be expected if the chelator is incorporated into both strands, in adjacent positions, termed

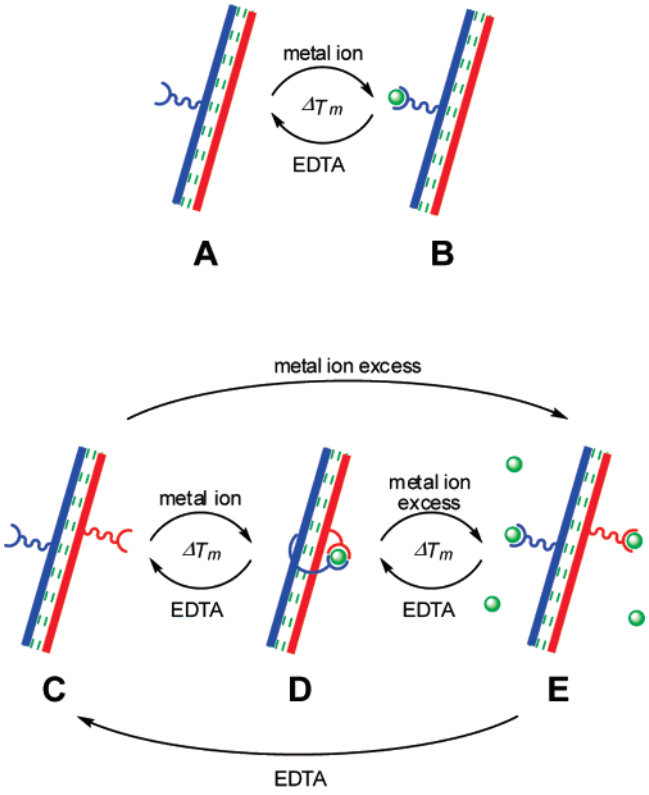

Figure 1. Mechanism of metal-induced modulation of duplex stability in an idealized system.

a "zipper" arrangement (Figure 1, structure C),[25] which could allow interstrand complexation (Figure 1, structure D) upon addition of 1 equiv of metal ion. Such linking between two complementary strands may provide additional stability to the duplex. On the other hand, in the presence of an excess of metal ion, the interstrand metal-ion-linked complex could disassemble, leading to the formation of functionalized duplexes (Figure 1, structure E), which may differ in stability from structures C and D. In principle, all the above-mentioned transitions can be reversed by removal of the added metal ion, e.g., by addition of EDTA.

Recently, we reported synthesis of an N2′-substituted 2′-amino-LNA[26] (LNA = locked nucleic acid) derivative functionalized with an *N*,*N*-bis(2-pyridylmethyl)-*β*-alanyl moiety located in the minor groove, which showed potential for changing DNA duplex stability, depending on the presence or absence of different divalent transition metal ions.[14] However, the ability of that system to form an interstrand complex (like Figure 1, structure D) was not extensively explored. Herein we

(12) Ono, A.; Togashi, H. *Angew. Chem. Int. Ed.* **2004**, *43*, 4300−4302.
(13) (a) Bashkin, J. K.; Frolova, E. I.; Sampath, U. *J. Am. Chem. Soc.* **1994**, *116*, 5981−5982. (b) Putnam, W. C.; Bashkin, J. K. *Chem. Commun.* **2000**, 767−768. (c) Matsumura, K.; Endo, M.; Komiyama, M. *J. Chem. Soc., Chem. Commun.* **1994**, 2019−2020. (d) Vlassov, V.; Abramova, T.; Godovikova, T.; Giege, R.; Silnikov, V. *Antisense Nucleic Acid Drug Dev.* **1997**, *7*, 39−42. (e) Magda, D.; Miller, R. A.; Sessler, J. L.; Iverson, B. L. *J. Am. Chem. Soc.* **1994**, *116*, 7439−7440. (f) Endo, M.; Azuma, Y.; Saga, Y.; Kuzuya, A.; Kawai, G.; Komiyama, M. *J. Org. Chem.* **1997**, *62*, 846−852. (g) Wei, L.; Babich, J.; Eckelman, W. C.; Zubieta, J. *Inorg. Chem.* **2005**, *7*, 2198−2209. (h) Åström, H.; Strömberg, R. *Nucleosides Nucleotides Nucleic Acids* **2001**, *20*, 1385−1388. (i) Åström, H.; Williams, N. H.; Strömberg, R. *Org. Biomol. Chem.* **2003**, *1*, 1461−1465. (j) Åström, H.; Strömberg, R. *Org. Biomol. Chem.* **2004**, *2*, 1901−1907. (k) Hall, J.; Hüsken, D.; Häner, R. *Nucleic Acids Res.* **1996**, *24*, 3522−3526. (l) Sakamoto, S.; Tamura, T.; Furukawa, T.; Komatu, Y.; Ohtsuka, E.; Kitamura, M.; Inoue, H. *Nucleic Acids Res.* **2003**, *31*, 1416−1425. (m) Roelfes, G.; Feringa, B. L. *Angew. Chem. Int. Ed.* **2005**, *44*, 3230−3232.
(14) Babu, R. B.; Hrdlicka, P. J.; McKenzie, C. J.; Wengel, J. *Chem. Commun.* **2005**, 1705−1707.
(15) Trawik, B. N.; Daniher, A. T.; Bashkin, J. K. *Chem. Rev.* **1998**, *98*, 939−960.
(16) Niittymäki, T.; Lönnberg, H. *Org. Biomol. Chem.* **2006**, *4*, 15−25.
(17) Martin, R. B. *Acc. Chem. Res.* **1985**, *18*, 32−38.
(18) Duguid, J.; Bloomfield, V. A.; Benevides, J.; Thomas, G. J., Jr. *Biophys. J.* **1993**, *65*, 1916−1928.
(19) Vliet, P. M.; Toekimin, S. M. S.; Haasnoot, J. G.; Reedijk, J.; Novakova, O.; Vrana, O.; Brabec, V. *Inorg. Chim. Acta* **1995**, *231*, 57−64.
(20) Clarke, M. J.; Zhu, F.; Frasca, D. R. *Chem. Rev.* **1999**, *99*, 2511−2533.
(21) Shin, A.; Eiichi, K. *Chem. Rev.* **2004**, *104*, 769−787.
(22) Zapata, L.; Bathany, K.; Schmitter, J.; Moreau, S. *Eur. J. Org. Chem.* **2003**, 1022−1028.
(23) Göritz, M.; Krämer, R. *J. Am. Chem. Soc.* **2005**, *127*, 18016−18017.
(24) Ossipov, D. A.; Strömberg, R. *Nucleosides Nucleotides Nucleic Acids* **2005**, *24*, 901−905.

(25) In this article we use the "zipper" nomenclature for naming different arrangements of complexing monomers in the duplexes. "*n* zipper" is a descriptor of the arrangement of two nucleosides of interest, positioned in *opposite* strands of duplex. Number *n* indicates the distance, measured in base pairs, between the two nucleosides, and it has a positive value if one nucleoside is shifted relative to the other toward the 5′-end (of its own strand), or a negative value if the nucleoside is shifted toward the 3′-end. Hence, the two **X** monomers in the duplex 5′-d(GTG A**X**A TGC):3′-d(CAC TA**X** ACG) are positioned in a "+1 zipper".

(26) (a) Singh, S. K.; Kumar, R.; Wengel, J. *J. Org. Chem.* **1998**, *63*, 10035−10039. 2′-Amino-LNA is defined in this article as an oligonucleotide containing at least one 2′-amino-2′-deoxy-2′-*N*,4′-*C*-methylene-*β*-D-ribofuranosyl nucleotide monomer. The O5′-DMT mono-protected 2′-amino-LNA nucleoside **4** was synthesized from the corresponding O3′-benzyl mono-protected nucleoside[26b] using procedures similar to those described for synthesis of the N2′-methylated derivative of nucleoside **4**.[26b,26c] (b) Rosenbohm, C.; Christensen, S. M.; Sørensen, M. D.; Pedersen, D. S.; Larsen, L.-E.; Wengel, J.; Koch, T. *Org. Biomol. Chem.* **2003**, *1*, 655. (c) Manuscript in preparation.

Scheme 1[a]

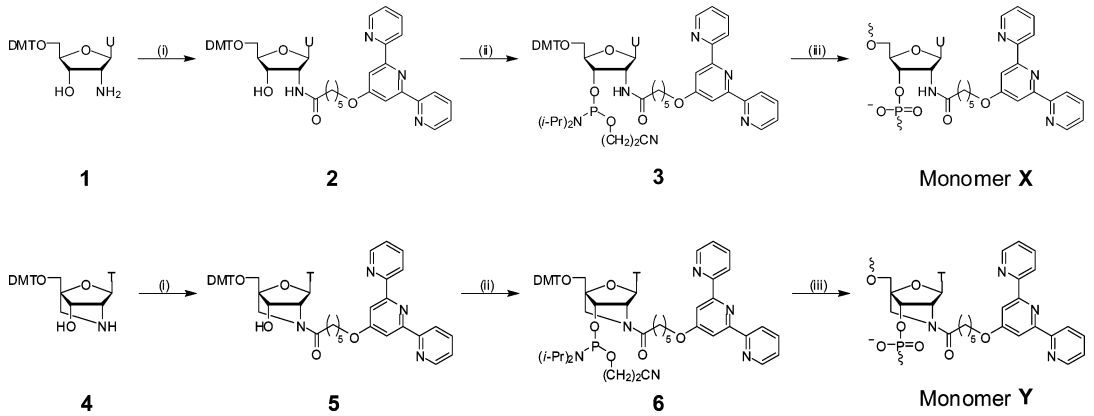

[a] Reagents and conditions: (i) 6-(2,2′:6′,2″-terpyridin-4′-yloxy)hexanoic acid, EDC·HCl, CH_2Cl_2 (**2**, 72%; **5**, 72%); (ii) $NC(CH_2)_2OP(Cl)N(i\text{-}Pr)_2$, $EtN(i\text{-}Pr)_2$, CH_2Cl_2 (**3**, 95%; **6**, 61%); (iii) DNA synthesizer. DMT = 4,4′-dimethoxytrityl. U = uracil-1-yl. T = thymin-1-yl

present a series of studies on conjugates of ONs with another high-affinity metal-chelating unit, namely 2,2′:6′,2″-terpyridine, which is known to effectively form 2:1 ligand-to-metal ion complexes.[9,22,23,27−30] The synthesis of two novel terpyridine-functionalized monomers, 2′-amino-2′-deoxyuridine monomer **X** and 2′-amino-LNA thymine monomer **Y**, is reported, and the properties of ONs containing these monomers are described in detail.

Results and Discussion

Synthesis. Phosphoramidite building blocks **3** and **6**, suitable for incorporation of monomers **X** and **Y** into ONs, were synthesized as shown in Scheme 1. EDC-promoted (EDC = 1-(3-dimethylaminopropyl)-3-ethylcarbodiimide) amide bond formation between the appropriate O5′-DMT-protected (DMT = 4,4′-dimethoxytrityl) nucleosides **1**[31] or **4**[26] and 6-(2,2′:6′,2″-terpyridin-4′-yloxy)hexanoic acid[32] gave intermediates **2** and **5**, respectively. Subsequent phosphitylation of the 3′-hydroxy group afforded the desired phosphoramidites **3** and **6** in 68% and 44% overall yields, respectively.

Synthesis of ONs containing monomer **X** or **Y** was performed on an automated DNA synthesizer following standard protocols (2 min coupling time, 1*H*-tetrazole as activator), except for slight modifications during coupling of phosphoramidites **3** and **6**.[33] To accomplish incorporation of monomer **X**, a double coupling procedure with an extended coupling time (2 × 30 min, 4,5-dicyanoimidazole as activator) was required, resulting in 85−90% stepwise coupling yield. This low coupling efficiency of phosphoramidite **3** is in agreement with earlier reports on low reactivity of 2′-amino-2′-deoxyuridine derivatives during ONs synthesis.[34,35] Monomer **Y** was incorporated in >98% stepwise coupling yield using an extended coupling time (30 min, 1*H*-tetrazole as an activator). All synthesized ONs were purified by RP-HPLC, and their compositions confirmed by MALDI-MS analysis (Table S1, Supporting Information).[33]

Thermal Denaturation Studies Involving 2′-Amino-DNA Monomer X. First, the effect of incorporation of monomer **X** on duplex stability in the absence or presence of Cu^{2+}, Zn^{2+}, and Ni^{2+} at different concentrations was evaluated by UV−thermal duplex denaturation studies using medium salt buffer (Table 1). When T_m measurements were carried out in the presence of EDTA, incorporation of a single monomer **X** into mixed-sequence 9-mer ONs (**ON1**−**ON6**) resulted in sequence-specific changes of thermal duplex stability, dependent on the type of nucleobase flanking monomer **X** at the 3′-side. When a purine monomer was present in this position (**ON1**, **ON2**, **ON5**), only slight duplex destabilization was observed (ΔT_m = −0.5 to −2.5 °C, relative to unmodified DNA:DNA duplexes of the same sequence), whereas the presence of a pyrimidine monomer (**ON3**, **ON4**, **ON6**) resulted in a considerable destabilization (ΔT_m = −8.5 to −11.0 °C). The latter effect is consistent with earlier observations, showing a decrease in duplex stability induced by 2′-amino-2′-deoxyuridine and its N2′-acylated derivatives.[36,37]

The relatively minor influence of monomer **X** on the thermal stability when flanked on the 3′-side by a purine monomer probably indicates some interaction between the terpyridine moiety and the adjacent nucleobase. Similar experiments were conducted with addition of 1 equiv or an excess (5 equiv and additionally 100 equiv for Ni^{2+}) of divalent transition metal ions. Increasing the transition metal ion concentration had no effect on the stability of unmodified DNA:DNA duplexes and almost no effect on the stability of duplexes formed between ONs containing monomer **X** flanked on the 3′-side with a pyrimidine nucleoside (**ON3**, **ON4**, **ON6**) and their DNA complements. In contrast, the presence of all tested divalent metal ions caused substantial destabilization (ΔT_m = −8.5 to −13.0 °C) of duplexes containing **ON1**, **ON2**, and **ON5**, having a purine monomer flanking monomer **X** at the 3′-side. T_m values observed in the presence of Cu^{2+}, Zn^{2+}, and Ni^{2+} were very similar in all tested sequence contexts and correspond to those reported

(27) Martin, R. B.; Lissfelt, J. A. *J. Am. Chem. Soc.* **1956**, *78*, 938−940.
(28) Holyer, R. H.; Hubbard, C. D.; Kettle, S. F. A.; Wilkins, R. G. *Inorg. Chem.* **1966**, *5*, 622−625.
(29) Cali, R.; Rizzarelli, E.; Sammartano, S.; Siracusa, G. *Transition Met. Chem.* **1979**, *4*, 328−332.
(30) Priimov, G. U.; Moore, P.; Helm, L.; Merbach, A. E. *Inorg. React. Mech.* **2001**, *3*, 1−23.
(31) McGee, D. P. C.; Vaughn-Settle, A.; Vargeese, C.; Zhai, Y. *J. Org. Chem.* **1996**, *61*, 781−785.
(32) Anders, P. R.; Lunkwitz, R.; Pabst, G. R.; Böhn, K.; Wouters, D.; Schmatloch, S.; Schubert, U. S. *Eur. J. Org. Chem.* **2003**, 3769−3776.
(33) See the Supporting Information.
(34) Hwang, J. T.; Greenberg, M. M. *Org. Lett.* **1999**, *1*, 2021−2024.
(35) Vargeese, C.; Carter, J.; Yegge, J.; Krivjansky, S.; Settle, A.; Kropp, E.; Peterson, K.; Pieken, W. *Nucleic Acids Res.* **1998**, *26*, 1046−1050.
(36) Kalra, N.; Babu, B. R.; Parmar, V. S.; Wengel, J. *Org. Biomol. Chem.* **2004**, *2*, 2885−2887.
(37) Kalra, N.; Parlato, M. C.; Parmar, V. S.; Wengel, J. *Bioorg. Med. Chem. Lett.* **2006**, *16*, 3166−3169.

Table 1. Thermal Denaturation Temperatures (T_m Values) of Duplexes Containing Monomer **X** Measured at Different Concentrations of Divalent Metal Ions[a]

			$+Cu^{2+}$		$+Zn^{2+}$		$+Ni^{2+}$		
code	sequence	+EDTA[b]	1 equiv[c]	5 equiv[c]	1 equiv[c]	5 equiv[c]	1 equiv[c]	5 equiv[c]	100 equiv[c]
ON1	5′-d(GTG A**X**A TGC)	26.5[d]	17.5[d]	17.0[d]	19.0[d]	19.5[d]	17.0[d]	16.5[d]	18.5[d]
DNA	3′-d(CAC TAT ACG)	(−1.5)	(−10.5)	(−11.0)	(−9.0)	(−8.5)	(−11.0)	(−11.5)	(−9.5)
ON2	5′-d(GTG A**X**G TGC)	33.0[d]	28.0[d]	28.5[d]	30.0[d]	29.5[d]	25.5[d]	29.5[d]	
DNA	3′-d(CAC TAC ACG)	(−2.5)	(−7.5)	(−7.0)	(−5.5)	(−6.5)	(−10.0)	(−6.0)	
ON3	5′-d(GTG A**X**T TGC)	20.5[d]	19.0[d]	20.0[d]	20.5[d]	20.0[d]	19.0[d]	19.0[d]	
DNA	3′-d(CAC TAA ACG)	(−11.0)	(−12.5)	(−11.5)	(−10.5)	(−11.5)	(−12.5)	(−12.5)	
ON4	5′-d(GTG A**X**C TGC)	25.5[d]	27.0[d]	27.5[d]	26.5[d]	27.5[d]	25.0[d]	26.5[d]	
DNA	3′-d(CAC TAG ACG)	(−8.5)	(−7.0)	(−6.5)	(−7.5)	(−6.5)	(−9.0)	(−7.5)	
DNA	5′-d(GTG ATA TGC)	27.5[d]	19.5[d]	19.5[d]	21.5[d]	21.0[d]	15.0[d]	17.5[d]	19.0[d]
ON5	3′-d(CAC TA**X** ACG)	(−0.5)	(−8.5)	(−8.5)	(−6.5)	(−7.0)	(−13.0)	(−10.5)	(−9.0)
DNA	5′-d(GTG ATA TGC)	22.0[d]	21.0[d]	21.0[d]	22.0[d]	22.5[d]	18.0[d]	18.5[d]	18.0[d]
ON6	3′-d(CAC **X**AT ACG)	(−6.0)	(−7.0)	(−7.0)	(−6.0)	(−5.5)	(−10.0)	(−9.5)	(−10.0)
ON7	5′-d(GT**G**^{L} A**X**A **T**^{L}GC)	36.5[d]	29.5[d]	29.5[d]	29.5[d]	30.5[d]	29.0[d]	30.0[d]	30.0[d]
DNA	3′-d(CAC TAT A CG)	(+8.5)	(+1.5)	(+1.5)	(+1.5)	(+2.5)	(+1.0)	(+2.0)	(+2.0)
DNA	5′-d(GTG ATA TGC)	36.5[d]	30.0[d]	29.5[d]	31.0[d]	31.0[d]	31.0[d]	30.5[d]	30.0[d]
ON8	3′-d(CAC **T**^{L}A**X** A^{Me}**C**^{L}G)	(+8.5)	(+2.0)	(+1.5)	(+3.0)	(+3.0)	(+3.0)	(+2.5)	(+2.0)
ON1	5′-d(GTG A**X**A TGC)	20.0[d]	20.0[d]	19.0[d]	32.5[d,e]	30.5[d,e]	46.5[d]	19.5[d]	22.5[d]
ON5	3′-d(CAC TA**X** ACG)	(−8.0)	(−8.0)	(−9.0)	(+4.5)	(+2.5)	(+18.5)	(−8.5)	(−5.5)
ON1	5′-d(GTG A**X**A TGC)	31.0[d]	34.5[d]	32.0[d]	53.5[d,e]	44.0[d,e]	56.5[d,e]	54.0[d]/ 31.0[e,g]	54.0[d] / 31.0[e,g]
ON8	3′-d(CAC **T**^{L}A**X** A^{Me}**C**^{L}G)	(+3.0)	(+6.5)	(+4.0)	(+25.5)	(+16.0)	(+28.5)	(+3.0)	(+3.0)
ON7	5′-d(GT**G**^{L} A**X**A **T**^{L}GC)	32.5[d]	36.0[d]	32.0[d]	55.5[d,e]	44.5[d,e]	53.0[d,e]	53.0[d]/ 33.0[e,g]	51.5[d]/ 33.5[e,g]
ON5	3′-d(CAC TA**X** ACG)	(+4.5)	(+8.0)	(+4.0)	(+27.5)	(+16.5)	(+25.0)	(+5.0)	(+5.5)
ON1	5′-d(GTG A**X**A TGC)	22.0[d]	34.0[d]	<10.0[d]	21.5[d]	18.5[d]	39.5[d,f]	40.5[d]/ 15.0[f,g]	12.5[d]
ON6	3′-d(CAC **X**AT ACG)	(−6.0)	(+6.0)		(−6.5)	(−9.5)	(+11.5)	(−13.0)	(−15.5)
ON7	5′-d(GT**G**^{L} A**X**A **T**^{L}GC)	29.0[d]	24.0[d]	24.5[d]	33.0[d,e]	32.5[d,e]	54.5[d]	19.5[d]	17.5[d]
ON6	3′-d(CAC **X**AT A CG)	(+1.0)	(−4.0)	(−3.5)	(+5.0)	(+4.5)	(+26.5)	(−8.5)	(−10.5)

[a] Thermal denaturation temperatures, T_m/°C; in parentheses are ΔT_m/°C, i.e., change in T_m value relative to unmodified DNA:DNA duplex of the same sequence. The T_m values of the unmodified duplexes or LNA-modified DNA duplexes were independent of divalent metal concentration and displayed the following values: 28.0 °C for **ON1**, **ON5**, and **ON6**, 35.5 °C for **ON2**, 31.5 °C for **ON3**, 34.0 °C for **ON4**, and 28.5 °C for **ON7** and **ON8**. T_m values were measured as the maximum of the first derivatives of the melting curves (A_{260} vs temperature) recorded in medium salt buffer (100 mM NaCl, adjusted to pH 7.0 with 10 mM NaH_2PO_4/5 mM Na_2HPO_4), using 1 μM concentrations of two complementary strands; T_m values are averages of at least two measurements. **G**^{L} = guanin-9-yl LNA monomer; **T**^{L} = thymin-1-yl LNA monomer; ^{Me}**C**^{L} = 5-methylcytosin-1-yl LNA monomer. See Scheme 1 for structure of monomer **X** (symbol "**X**" was used in the table for clarity). [b] [EDTA] = 0.1 mM. [c] M^{2+} equivalents relative to duplex. [d] Sample denaturized for 1 min at 80 °C before measurement. [e] Sample denaturized for 15 min at 80 °C before measurement. [f] Sample denaturized for 30 min at 80 °C before measurement. [g] Strands premixed separately with Ni^{2+} solution, and sample then denaturized for 1 min at 80 °C before measurement.

for other 2′-amino-2′-deoxyuridine-modified duplexes,[37] further supporting the hypothesis of some favorable interaction between the terpyridine moiety and a 3′-flanking purine nucleobase. Upon metal complexation, this interaction is apparently broken, resulting in destabilization and a 5−10 °C decrease in the T_m value, relative to that of unmodified standard. Circular dichroism (CD) spectroscopy was employed to determine if some differences in duplex structure could be observed upon metal complexation with either a purine (**ON1**:DNA) or a pyrimidine (**ON3**:DNA) flanking monomer at the 3′-side of monomer **X**. There was no visible difference in the CD spectra, neither with nor without Ni^{2+}, and in all cases a typical B-type duplex CD pattern was observed (Figures S16 and S17, Supporting Information).[33]

To test if the overall rigidity of the duplex and its conversion from B-type to a more A-type-like structure may influence the effect of metal-induced stability change, ONs containing monomer **X** (3′-flanked with A) and two LNA monomers (**ON7**, **ON8**) were used in thermal denaturation studies.[38] Duplexes formed between these ONs and their DNA complements, in the absence of transition metal ions, were stabilized (ΔT_m = +8.5 °C) to an extent expected for two LNA monomers being incorporated.[39] Upon addition of divalent metal ions, the T_m values decreased between 5.5 and 7.5 °C, indicating that the metal-induced destabilizing effect is still present, however, to a smaller degree than observed for **ON1**−**ON6**.

Duplexes Having Monomer X in Both Strands. (a) The "+1 Zipper" System. To establish if monomer **X** can be used for duplex stability modulation in the way presented in Figure 1, duplexes formed with two complementary 9-mers, each containing a single incorporation of monomer **X**, were studied. When the two monomers **X** were positioned in a "+1 zipper" (**ON1**:**ON5**) constitution, addition of 1 equiv of Ni^{2+} resulted in a remarkable increase in duplex stability (ΔT_m = +26.5 °C, relative to **ON1**:**ON5** measured with EDTA; ΔT_m = +18.5 °C, relative to unmodified DNA:DNA). Similarly, the presence of 1 equiv of Zn^{2+} led to a thermal stabilization of the duplex, but to a lesser extent (ΔT_m = +12.5 °C, relative to the EDTA experiment), whereas Cu^{2+} had no effect. On the other hand, an excess of Ni^{2+} resulted in a thermal stability similar to that obtained in the EDTA experiment. An excess of Zn^{2+} caused

(38) Petersen, M.; Nielsen, C. B.; Nielsen, K. E.; Jensen, G. A.; Bondensgaard, K.; Singh, S. K.; Rajwanshi, V. K.; Koshkin, A. A.; Dahl, B. M.; Wengel, J.; Jacobsen, J. P. *J. Mol. Recognit.* **2000**, *13*, 44−53.

(39) Hrdlicka, P. J.; Babu, B. R.; Sørensen, M. D.; Harris, N.; Wengel, J. *J. Am. Chem. Soc.* **2005**, *127*, 13293−13299.

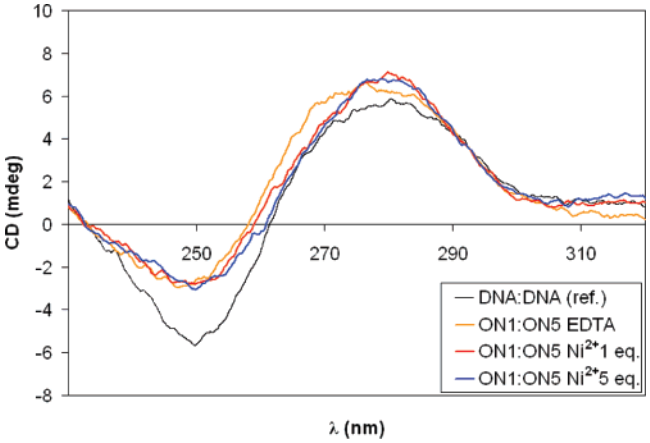

Figure 2. Comparison of CD spectra of duplex containing two **X** monomers in "+1 zipper" constitution in the absence or presence of different equivalents of Ni^{2+}. The spectra were recorded at 10 °C, otherwise using the same experimental conditions as used during thermal denaturation experiments.

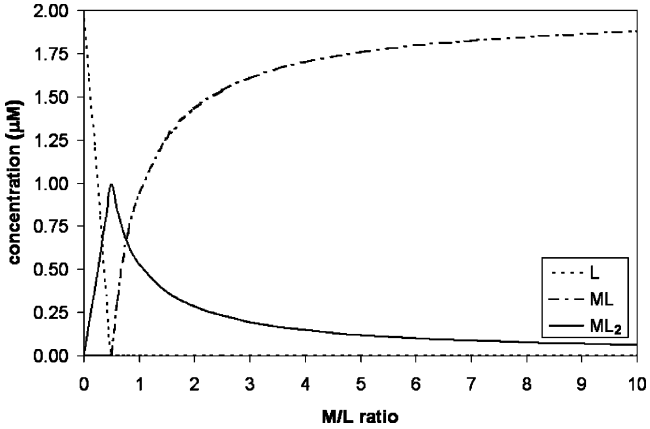

Figure 3. Distribution of the species in solution containing 2,2′:6′,2″-terpyridine and Ni^{2+}. L, terpyridine; ML, $Ni(terpy)^{2+}$; ML_2, $Ni(terpy)_2^{2+}$.

only a small decrease in duplex stability relative to the case when 1 equiv of metal ion was used, but the T_m value still remained 10.5 °C higher than that obtained when EDTA was present. As the stability of the M^{2+}:terpy complexes in general is expected to follow the order $Ni^{2+} > Cu^{2+} > Zn^{2+}$,[28,29] these results indicate that an appropriate geometry for interstrand terpy:Ni^{2+}:terpy bridging (see molecular modeling below) can be adopted for 1 equiv of Ni^{2+}, but not for Cu^{2+}. The Ni^{2+}-bridging likely involves two terpyridine ligands and octahedral coordination, which might not be the case for the Cu^{2+} system (less than six electron-donating ligand groups are generally preferred). CD spectra of the "+1 zipper" system, recorded in the absence and presence of different amounts of Ni^{2+}, revealed in all cases curves very similar to the unmodified reference, indicating a typical B-type duplex structure (Figure 2). In the experiments described above, the thermodynamically most stable complexes are analyzed, but it should be noted that the opportunity exists that terpy:M^{2+}:terpy complex formation precedes duplex formation during all the zipper experiments in the presence of M^{2+} ions.

The same "+1 zipper" arrangement of monomer **X** was studied with two additional LNA monomers incorporated in one of the strands (**ON1**:**ON8** and **ON7**:**ON5**). The trends observed were essentially similar to those for **ON1**:**ON5**, with almost identical differences in T_m values between measurements with EDTA, 1 equiv of metal ion, and excess metal ion when Cu^{2+} or Ni^{2+} was used, but with a more pronounced effect for Zn^{2+}.

Collectively, the observations described above suggest that two **X** monomers located in opposite strands in a "+1 zipper" constitution are able to form a stabilizing, metal-linked bridge outside the duplex core, as depicted in Figure 1 (structure D). Furthermore, the addition of metal ions, even when putatively leading to the assembly of the interstrand linkage, does not disturb the native B-type structure of the duplex. Finally, the results suggest that this linkage is not formed if metal ions are present in excess, which can be explained by the formation of a less stable structure (Figure 1, structure E). However, T_m values observed under an excess of metal ions suggest that two positively charged M^{2+}:terpy complexes can probably occupy positions distant from each other, so that no destabilizing effect is observed.

Although the thermal stability of the duplexes upon introduction of the two LNA units did not change very much, major differences were observed in the kinetic behavior of the "+1 zipper" system in the presence of an excess of Ni^{2+}. During initial thermal denaturation experiments, carried out with both 5 and 100 equiv of Ni^{2+}, following the same experimental protocol used up to this point, measured T_m values were almost identical to those obtained when 1 equiv of Ni^{2+} was used (54.0 °C for **ON1**:**ON8** and 53.0 or 51.5 °C for **ON7**:**ON5**). This suggested that the high-melting metal ion "cross-linked" structure (Figure 1, structure D) was persistent even in the presence of a large Ni^{2+} excess. To get some insight into this phenomenon, we investigated available thermodynamic and kinetic data concerning Ni^{2+}:terpy complexes.[28] From the graph of the theoretical $Ni(terpy)^{2+}$ and $Ni(terpy)_2^{2+}$ distribution versus Ni^{2+} amount (Figure 3), plotted using cumulative complex stability constants,[35] it is clear that, at 2.5 equiv of Ni^{2+} per ligand (5 equiv per duplex containing two terpyridines), and especially at 50 equiv (100 equiv per duplex), the dominating species would be expected to be the 1:1 complex (corresponding to Figure 1, structure E). Therefore, we consider the basis of the observed results to be the kinetic stability of the terpy:Ni^{2+}:terpy complex (Figure 1, structure D). Indeed, the activation energy of this complex dissociation is relatively high (20.8 kcal/mol), and its half-life can be calculated to be 104 h at 25 °C and 25 min at 80 °C.[28] Even though these values are calculated for free, nonconjugated terpyridine, they indicate that the standard 1 min denaturation protocol, which is enough for normal DNA duplex denaturation, was not adequate to investigate the system with two 1:1 complexes (Figure 1, structure E) and that the sample in this case should be denatured for a longer period.

Figure 4 depicts three thermal denaturation curves registered from samples prepared by mixing **ON1** and **ON8** in the buffer, followed by addition of 100 equiv of Ni^{2+} and denaturation at 80 °C for 1, 6, and 15 min, respectively. Comparison of these curves clearly shows transformation from a high-melting form (1 min denaturation) to a low-melting form (15 min denaturation), with two transitions observed using 6 min denaturation. Formation of the bridged structure (Figure 1, structure D) is indicated to be the kinetic product upon Ni^{2+} addition—probably facilitated by the preorganization of the terpyridine ligands in the duplex structure. This high-T_m transition should be eliminated if the Ni^{2+}:terpy (1:1) complexes (Figure 1, structure E)

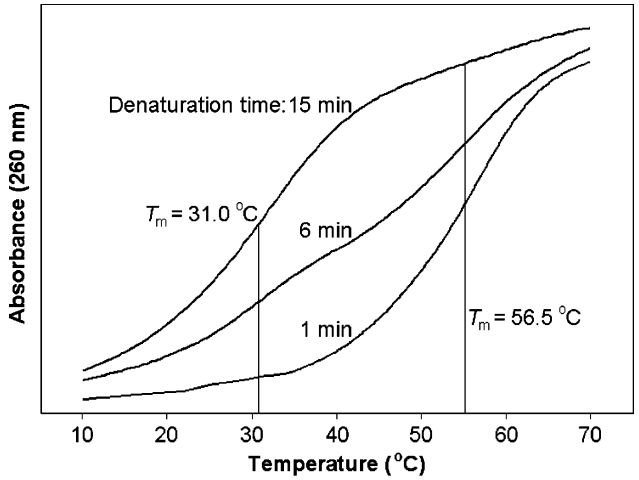

Figure 4. Thermal denaturation curves of **ON1**:**ON8** duplex in the presence of excess Ni^{2+} (100 equiv), measured after different denaturation times. Oligonucleotides were mixed prior to addition of Ni^{2+} solution and denaturation.

are formed before duplex assembly. Indeed, when the DNA strands (**ON1** and **ON8**, or **ON7** and **ON5**) were first separately premixed with an excess of Ni^{2+}, denatured for only 1 min, and then hybridized, the thermal denaturation curves showed only a single transition at the lower denaturation temperature.

(b) The "1 Zipper" System. Having characterized the "+1 zipper" constitution of monomer **X**, we moved to the "−1 zipper" constitution (**ON1**:**ON6**). In this case, when no transition metal ion was present, duplex stability was affected to more or less the same extent ($\Delta T_m = -6$ °C, relative to unmodified reference) as for the "+1 zipper". With 1 equiv of Cu^{2+} and Ni^{2+}, an increase in the T_m value was observed ($\Delta T_m = +6$ and +11 °C, respectively), whereas an excess of these metal ions caused significant duplex destabilization ($\Delta T_m = -24$ to −27 °C when compared with having only 1 equiv of metal ion), testified by T_m values more than 10 °C below the "no-metal" (EDTA experiment) level. Interestingly, when 5 equiv of Ni^{2+} was used, prolonged denaturation time or premixing the strands with Ni^{2+} had to be applied to obtain a single melting curve transition (appearing at the "low" temperature). Additional incorporation of two LNA monomers into one of the strands (**ON7**:**ON6**) led to complete disappearance of the Cu^{2+}-induced effects, but the specific influence of Ni^{2+} on duplex stability was even more pronounced. Notably, the difference in T_m values between the experiment with 1 equiv of Ni^{2+} and that with an excess of Ni^{2+} rose to 35 °C, and the kinetic persistence of this particular interstrand complex (Figure 1, structure D) under excess metal ion conditions decreased, giving the "low-melting" form even with only 1 min denaturation time. That a similar kinetic effect is not observed with Cu^{2+} (e.g., **ON1**:**ON6**) might be due to the ability of Cu^{2+} complexes to undergo rapid constitutional and conformational changes. A characteristic feature of the "−1 zipper" system, not present in the "+1 zipper" arrangement, is a relatively strong destabilizing effect of an excess of Ni^{2+} and Cu^{2+} ions. Such an effect might result from repulsion of two positively charged M^{2+}:terpy complexes. This would mean that, contrary to the situation in the "+1 zipper" constitution, the two complexes are placed in close proximity, which forces them to interfere.

The obtained results clearly show that there are strict spatial requirements for formation of interstrand linkages for different metal ions. Ni^{2+} is able to produce such a complex in both "+1 zipper" or "−1 zipper" constitutions, and in the presence of absence of additional LNA monomers. A terpy:Cu^{2+}:terpy complex seems to be formed only in the "−1 zipper" arrangement, but only when no LNA units are incorporated, whereas Zn^{2+} tolerates "+1 zipper" exclusively. The differences probably arise from different stabilities of octahedral terpy:M^{2+}:terpy complexes. Formation of a very thermodynamically stable Ni^{2+} complex apparently compensates any associated unfavorable changes in the duplex structure, therefore still leading to duplex stabilization. In case of Cu^{2+} and Zn^{2+}, the energy gained during complexation is more limited, therefore allowing interstrand metal-linked complex formation only in certain cases.

Studies Involving 2′-Amino-LNA Monomer Y. Table 2 summarizes thermal denaturation results obtained with ONs containing 2′-amino-LNA-based monomer **Y**. For a number of applications, 2′-amino-LNA has proved to be advantageous due to its specific properties, including (a) locked 3′-endo furanose

Table 2. Thermal Denaturation Temperatures (T_m Values) of Duplexes Containing Monomer **Y** Measured at Different Concentrations of Divalent Metal Ions[a]

			+Cu^{2+}		+Zn^{2+}		+Ni^{2+}		
code	sequence	+EDTA[b]	1 equiv[c]	5 equiv[c]	1 equiv[c]	5 equiv[c]	1 equiv[c]	5 equiv[c]	100 equiv[c]
ON9	5′-d(GTG A**Y**A TGC)	35.0[d]	37.0[d]	36.0[d]	39.5[d]	40.0[d]	35.5[d]	38.5[d]	40.5[d]
DNA	3′-d(CAC TĀT ACG)	(+7.0)	(+9.0)	(+8.0)	(+11.5)	(+12.0)	(+7.5)	(+10.5)	(+12.5)
DNA	5′-d(GTG ATA TGC)	36.0[d]	38.0[d]	39.0[d]	39.5[d]	39.5[d]	42.0[d]	41.5[d]	41.0[d]
ON10	3′-d(CAC TA**Y** ACG)	(+8.0)	(+10.0)	(+11.0)	(+11.5)	(+11.5)	(+14.0)	(+13.5)	(+13.0)
DNA	5′-d(GTG ATA TGC)	36.5[d]	31.5[d]	31.5[d]	34.0[d]	32.5[d]	31.5[d]	32.0[d]	33.5[d]
ON11	3′-d(CAC **Y**AT ACG)	(+8.5)	(+3.5)	(+3.5)	(+6.0)	(+4.5)	(+3.5)	(+4.0)	(+5.5)
ON9	5′-d(GTG A**Y**A TGC)	49.0[d]	42.0[d]	43.0[d]	65.5[d]	55.5[d]	77.0[d,c]	76.0;44.0[d,e]/ 43.5[g,h]	74.5;45.5[d,e]/ 44.0[f,h]
ON10	3′-d(CAC TĀ**Y** ACG)	(+21.0)	(+14.0)	(+15.0)	(+37.5)	(+27.5)	(+49.0)	(+15.5)	(+16.0)
ON9	5′-d(GTG A**Y**A TGC)	41.0[d]	41.5[d]	42.5[d]	44.0[d]	46.5[d]	44.0[d]	42.0[d]	42.0[d]
ON11	3′-d(CAC **Y**ĀT ACG)	(+13.0)	(+13.5)	(+14.5)	(+16.0)	(+18.5)	(+16.0)	(+14.0)	(+14.0)

[a] Thermal denaturation temperatures, T_m/°C; in parentheses are ΔT_m/°C, i.e., change in T_m values relative to unmodified DNA:DNA duplex of the same sequence. T_m value of unmodified duplex was independent of divalent metal concentration and displayed the value of 28.0 °C. T_m values were measured as the maximum of the first derivatives of the melting curve (A_{260} vs temperature) recorded in medium salt buffer (100 mM NaCl, adjusted to pH 7.0 with 10 mM NaH_2PO_4/5 mM Na_2HPO_4), using 1 μM concentrations of two complementary strands; T_m values are averages of at least two measurements. See Scheme 1 for structure of monomer **Y** (symbol "**Y**" was used in the table for clarity). [b] [EDTA] = 0.1 mM. [c] M^{2+} equivalents relative to duplex. [d] Sample denaturized for 1 min at 80 °C before measurement. [e] Two transitions observed. [f] Sample denaturized for 15 min at 80 °C before measurement. [g] Sample denaturized for 30 min at 80 °C before measurement. [h] Strands premixed separately with Ni^{2+} solution, and sample then denaturized for 1 min at 80 °C before measurement.

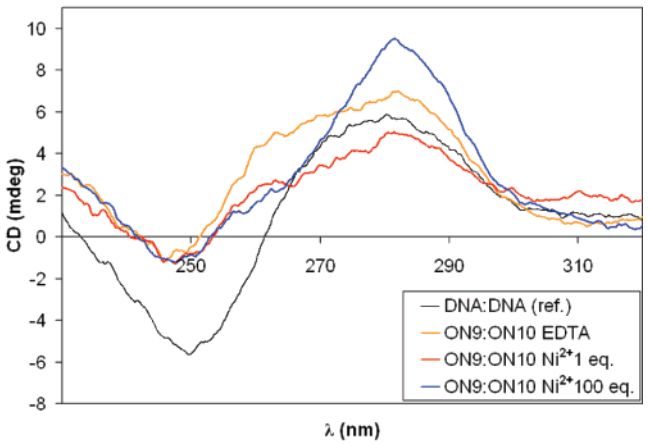

Figure 5. Comparison of CD spectra of duplex **ON9**:**ON10** containing two **Y** monomers in "+1 zipper" constitution, in the absence or presence of different equivalents of Ni^{2+}.

conformation, (b) improved binding toward DNA and RNA, (c) pronounced mismatch discrimination, and (d) precise positioning of N2′-substituents.[14,26,39] When a single monomer **Y** was incorporated into the 9-mer duplex (**ON9**−**ON11** toward DNA), thermal denaturation studies, carried out in the presence of EDTA, showed a thermal stabilization characteristic for singly modified LNA duplexes (ΔT_m = +7.0 to +8.5 °C, relative to unmodified reference). Addition of divalent metal ions resulted in only moderate changes in the melting temperatures (ΔT_m = −5.0 to +6.0 °C, relative to "no-metal" level).

Further extending our investigation of the LNA−metal chelator conjugate, we found that, when two monomers **Y** were positioned in a "+1 zipper" constitution (**ON9**:**ON10**), the presence of 1 equiv of Ni^{2+} resulted in unprecedented duplex stabilization (ΔT_m = +49.0 °C, relative to unmodified reference and ΔT_m = +28 °C compared to the EDTA experiment). To the best of our knowledge, this is the highest stabilizing effect observed with DNA−metal complex conjugates, and probably also the most efficient duplex stabilization effect ever reported. Likewise, addition of 1 equiv of Zn^{2+} resulted in a remarkable increase in thermal stability (ΔT_m = +37.5 °C, relative to unmodified reference and ΔT_m = +16.5 °C compared to the EDTA experiment), whereas Cu^{2+} had only a minor effect. Under excess Ni^{2+} conditions, the T_m value decreased to 5 °C below the "no-metal" level, which corresponds to a ΔT_m value of −33 °C when compared to the one-equivalent experiment. Additionally, following the trends observed with monomer **X**, increased kinetic stability of the interstrand bridged structure was observed, and to obtain melting curves with a single transition, prolonged denaturation time or premixing stands with Ni^{2+} had to be applied. Excess Zn^{2+} conditions resulted in a ΔT_m value of +6.5 °C when compared with the "no-metal" conditions. In summary, the monomer **Y** "+1 zipper" shows general properties very similar to those of the monomer **X** "+1 zipper" neighbored by two LNA nucleotides. This can be explained by conformational tuning of the monomer **X** (from C2′-endo toward C3′-endo conformation), as observed earlier for other 2′-amino-LNA/DNA strands.[36] Furthermore, the observed behavior is even more pronounced for the monomer **Y** than for monomer **X** in the LNA-modified DNA strands.

To obtain additional insight into the structure of this system, CD spectroscopy was employed (Figure 5). For all cases, CD curves indicate an intermediate A/B-type duplex structure, however, showing the closest resemblance to the B-type. In contrast to the monomer **X** "+1 zipper" system, the monomer **Y** "+1 zipper" system displayed nonidentical CD spectra with different equivalents of Ni^{2+}. This indicates that the terpy:Ni^{2+}:terpy complex (Figure 1, structure D) and the form with two Ni^{2+}:terpy (1:1) complexes (Figure 1, structure E) in this case display differences in overall duplex geometry.

Finally, two monomers **Y** in "−1 zipper" constitution were studied. Surprisingly, virtually no metal-induced effects were observed in this case. Probably the rigidity of the LNA backbone makes assembly of the interstrand complex (Figure 1, structure D) impossible, at least with the linker length applied.

Molecular Modeling. To rationalize the obtained results, in particular the differences observed between the two tested zipper constitutions, we performed simplified molecular modeling of selected duplexes containing the Ni^{2+} complex-bridged structure (**ON1**:**ON5**, **ON1**:**ON6**, **ON9**:**ON10**, and **ON9**:**ON11**). As CD spectroscopy revealed an overall B-type duplex geometry for **ON1**:**ON5** both without and in the presence of Ni^{2+}, the four duplexes were build as B-type duplexes. No attempt was made to modify the overall geometry of the LNA duplexes toward a more A-type geometry. Due to lack of AMBER force field parameters for the divalent transition metal ions, the structure of the octahedral $Ni(terpy)_2^{2+}$ complex was constrained according to available X-ray diffraction data.[40] Monte Carlo conformational analysis was performed, and the lowest energy structures were subjected to molecular dynamics followed by energy minimization using the AMBER force field[41] as implemented in MacroModel V.9.1.[42]

The lowest energy structure of the 9-mer duplex containing monomers **X** arranged in "+1 zipper" constitution (**ON1**:**ON5**, Figure 6) suggests that the complex occupies a well-adapted position in the minor groove. Formation of this interstrand linkage does not disturb the duplex structure in any way. A very similar picture is observed in the structure of the "+1 zipper" system formed with two **Y** monomers (**ON9**:**ON10**, Figure 6), with the bridging complex fitting perfectly into the minor groove. In contrast, in the "−1 zipper" constitution (**ON1**:**ON6** and **ON9**:**ON11**, Figure 6; 9-mers with monomer **X** and **Y**, respectively), the attachment points of the chelators are positioned in very close proximity. This structural feature makes formation of the interstrand complex inside the minor groove significantly more difficult. As a consequence, the terpyridine moieties must extend out of the duplex, and the complex has to be assembled outside the helix cylinder. Even though this structural arrangement is not as favorable as the well-adapted complex in the "+1 zipper" structure, thermal denaturation data indicate that it can be realized when monomer **X** is used (**ON1**:**ON6**), as manifested by the significant duplex stabilization observed. However, in the case of the far more rigid monomer **Y**, even though the lowest energy structure obtained from molecular modeling suggests that formation of this complex should also be possible, experimental results strongly indicate that no such complex is formed (**ON9**:**ON11**). From this we

(40) Baker, A. T.; Craig, D. C.; Rae, A. D. *Aust. J. Chem.* **1995**, *48*, 1373−1378.
(41) (a) Weiner, S. J.; Kollman, P. A.; Case, D. A.; Singh, U. C.; Ghio, C.; Alagona, G.; Profeta, S.; Weiner, P. *J. Am. Chem. Soc.* **1984**, *106*, 765−784. (b) Weiner, S. J.; Kollman, P. A.; Nguyen, D. T.; Case, D. A. *J. Comput. Chem.* **1986**, *7*, 230−252.
(42) *MacroModel*, version 9.1, Schrödinger, LLC, New York, NY, 2005.

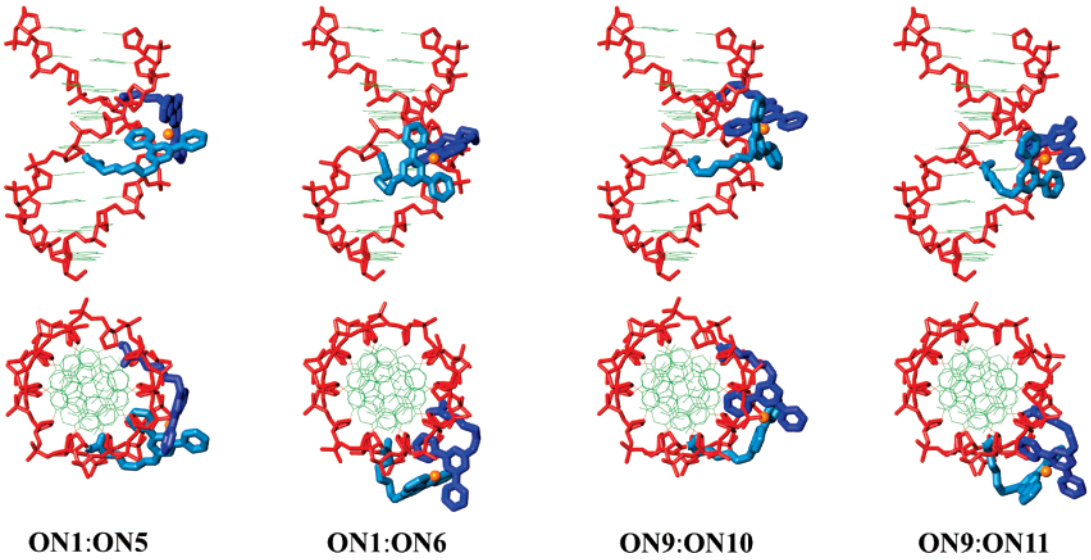

Figure 6. Lowest energy structure of the nucleic acid−metal complexes. Hydrogen atoms, sodium ions, and bond orders have been omitted for clarity. Color scheme: green, nucleobases; red, sugar−phosphate backbone; blue, N2′-functionalities; orange, nickel ion.

conclude that the structure observed from molecular modeling reflects a high-energy structure not accessible under the experimental conditions and, as such, being a consequence of the restrictions under which the molecular modeling was carried out.

Duplex Stability Modulation. Having characterized the different arrangements of monomers **X** and **Y** with varied amounts of the three divalent transition metal ions, we moved to study the practical possibilities of using our systems to modulate the duplex stability in the manner depicted in Figure 1. For the modulation mechanism shown in the upper part of Figure 1 (A↔B transitions), monomer **X** 3′-flanked with adenosine seemed to be the most suitable choice, since addition of divalent metal ion was associated with the most pronounced change in the T_m value. Indeed, a series of sequential thermal denaturation experiments using the **ON1**:DNA duplex, starting without any metal ions (T_m = 26.5 °C), followed by addition of 2 equiv of Ni^{2+} (T_m = 17.0 °C), followed by alternating additions of 4 equiv of EDTA (T_m = 26.5 °C) and 4 equiv of Ni^{2+} (T_m = 17.0 °C), proved the full reversibility of the process. Both Ni^{2+} and EDTA were added after finishing one denaturation process, and the sample was not denaturized before starting the next experiment. Similar results were obtained with the **ON5**:DNA duplex.

Next, we examined the possibility of more efficient T_m modulation using the zipper systems. In all cases tested (**ON1**:**ON5**, **ON1**:**ON6**, **ON1**:**ON8**, **ON7**:**ON5**, **ON7**:**ON6**, and **ON9**:**ON10** with Ni^{2+}; **ON1**:**ON8**, **ON7**:**ON5**, and **ON9**:**ON10** with Zn^{2+}; **ON1**:**ON6** with Cu^{2+}), it was possible to induce an increase in duplex stability by addition of 1 equiv of the metal ions (Figure 1, C→D transition) without denaturation of the sample. To reverse this process (Figure 1, D→C), 5 equiv of EDTA had to be added and the sample had to be denaturized for 5−30 min, depending on the sequence and metal ion used. The requirement for such long denaturation times is probably caused by the high kinetic stabilities of the terpy:M^{2+}:terpy complexes (Figure 1, structure D), combined with the unfavorable interactions between the negatively charged EDTA molecule and the negatively charged duplex when approaching each other. After EDTA treatment, we were not able to fully restore

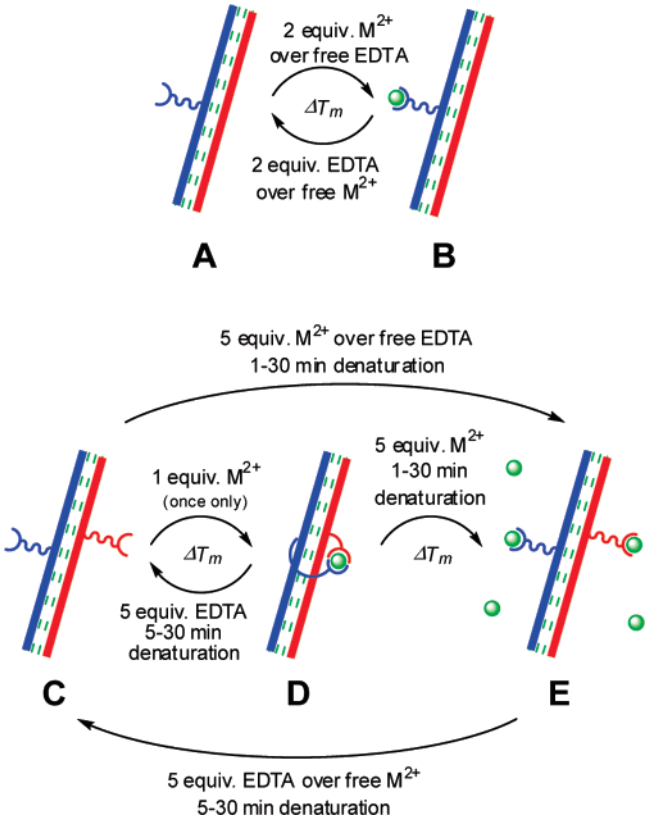

Figure 7. Overview of possible ways to modulate T_m using ONs containing monomers **X** and **Y**.

the high-melting bridged structure by addition of 5 equiv more of metal ions (Figure 1, C→D, for the second time), and only thermal denaturation curves containing double transitions were observed.

In the next series of experiments, the possibility of disassembly of the interstrand bridging complex by addition of excess metal ion (Figure 1, D→E) was studied. The obtained results are in perfect agreement with those reported in Tables 1 and 2, and all samples had to be denaturized for 1−30 min to achieve this transition. Again, we found it practically impossible to return

to the highly stabilized bridged structure (Figure 1, E→D) by addition of an appropriate amount of EDTA.

Finally, four examples showing significantly different thermal stability between "no-metal" and excess metal ion conditions (**ON1**:**ON6** with Ni^{2+} and Cu^{2+}; **ON1**:**ON8** and **ON7**:**ON5** with Zn^{2+}) were analyzed. To achieve the "no-metal" to excess metal transition (Figure 1, C→E, 5 equiv of M^{2+}), sample denaturation for 1−30 min (depending on the sequence and metal ion used) had to be applied. To reverse the process (Figure 1, situation E→C), at least 10 equiv of EDTA had to be added, and the sample had to be denaturized for 5−30 min. Unless these conditions were applied, multiple transitions, including high-temperature ones originating form the interstrand complex formation, were observed. However, the described transitions (C↔E) could be repeated several times by cumulative addition of 5 equiv of metal ions over free EDTA present in the sample (C→E) and addition of 5 equiv of EDTA over free metal ions (E→C) and combining these with denaturation. Figure 7 summarizes the possible ways of metal-mediated duplex stability modulation in the developed system, including the conditions required.

Conclusion

Development of methods that allow engineering of DNA duplex stability is desirable for possible applications in nanotechnology. Herein we have demonstrated a new strategy to achieve this aim by development of nucleic acid−metal chelator conjugates that allow unprecedented changes in duplex stability, depending on the presence or absence of divalent transition metal ions in various molar equivalents relative to nucleic acid duplex. Molecular modeling strongly suggests that the observed extraordinary T_m modulation is induced by interstrand metal complex formation in the minor groove of the duplex. Furthermore, practical aspects of system operation and dynamics have been studied.

Acknowledgment. We greatly appreciate funding from the Danish National Research Foundation and the Oticon Foundation. This work was supported by Sixth Framework Programme Marie Curie Host Fellowships for Early Stage Research Training, under contract no. MEST-CT-2004-504018.

Supporting Information Available: Synthetic experimental procedures; NMR spectra of compounds **2**, **3**, **5**, and **6**; experimental protocols for ON synthesis and purification, thermal denaturation studies, CD measurements, and molecular modeling; MALDI-TOF results for synthesized ONs; representative examples of thermal denaturation curves; details of calculation of the distribution of Cu^{2+}, Zn^{2+}, and Ni^{2+}–terpyridine complexes together with appropriate graphs for Cu^{2+} and Zn^{2+} (PDF); structural files (cf. Figure 6) (PDB). This material is available free of charge via the Internet at http://pubs.acs.org.

JA071076Z